A statistical deformation analysis of two epochs of terrestrial laser data of a lock

Roderik Lindenbergh and Norbert Pfeifer
Delft Institute of Earth Observation and Space systems
Delft University of Technology
R.C.Lindenbergh@lr.tudelft.nl

Abstract
Terrestrial laser scanning is a new method for monitoring deformation of complicated industrial objects. Deformation that is large compared to the measurement accuracy will be easy to track. In this study however, we compare scans of an object, a lock in the sea entrance of the Amsterdam harbor, were the possible deformation is in the order of the measurement noise. Two scans were obtained without physically changing the position of the scanner. We first show that the two resulting data sets still do not match over the entire scene. For further automated processing segmentation is performed, grouping the points into sets of planes describing the lock doors. Then we show how corresponding segments can be compared using the method of deformation analysis.

Keywords: terrestrial laser scanning, adjustment and testing theory, deformation monitoring

1. Introduction

Terrestrial laser scanning has matured and proven a suitable technology for acquiring data for cultural heritage/architecture and large scale topographic applications. Other examples include e.g. forestry [1]. These fields are characterized by accuracy requirements in the order of 1cm to 2cm. Also in industrial site modeling/reconstruction with tighter accuracy requirements it has proven to be a useful technique. This field is characterized by very regular shapes (cylinders, boxes, etc.) and accuracy requirements can be met because of the high over-determination due to the dense point cloud acquired. These applications were mainly tackled with photogrammetric approaches before the advent of terrestrial laser scanning.

Other fields of geodetic engineering, e.g. monitoring of structures and their deformation, are still performed rather with tacheometers than with terrestrial laser scanners. Deformation of (concrete and wooden) beams was studied with terrestrial laser scanners in [2]. Tunnel monitoring is discussed in [3] and [4]. In [5] the Leica HDS2500 was used to detect lock door deformation due to water pressure. Measurements were compared to tacheometric measurements and differences occurred of up to 3mm. By means of the high spatial resolution of the laser measurements it turned out to be possible to detect deformations ranging from 1.5cm to 4cm on the lock doors between high and low water pressure. In this paper we study the suitability of terrestrial laser scanning in a setup less controlled than e.g. the one of [2].

A **terrestrial laser scanner** determines the distance between a large number of object points and the scanner by emitting laser pulses in different directions and detecting the echoes from the objects. So called pulsed scanners measure the round trip travel time of the pulse towards an object and back. An overview of measurement techniques and scanner specifications can be found in [6]. In a performance comparison test of several scanners [7], measurement noise of terrestrial laser scanning was found to be between 1mm and 5mm at a scan distance of 90m for the Leica HDS 2500, the scanner we used.

In the **project** we performed an experiment with the Leica HDS2500 at a small sea-lock (Fig. 1) in IJmuiden that connects the main shipping channel from Amsterdan to the open North Sea. Two scans were obtained in a short time interval, the scan position was unchanged. At the moment of scanning the second scan, the water level behind the scanned lock door was about one meter higher than during the first scan. At the moment of scanning it was unclear if this change in water level would cause any deformation on the lock door.

The pulsed scanner used in the experiment described here is the **Leica HDS2500.** The company claims a precision of 6mm at a scan distance of 50m. The maximal scan distance amounts to 100m. The modeled surface precision according to Leica can be up to 2mm. The scan range is restricted to a scan window with an extent of both 40° in the vertical and the horizontal direction. Additionally to the *xyz*-location of the reflecting surface point, the intensity of the received echo is recorded as are three RGB color parameters by means of an internal camera.

Paper outline: In Section 2 we discuss the methods used for the data analysis as performed in Section 3. The methods include segmentation (2.1), direct comparison of measures points (2.2), analysis of movement for the entire scene (2.3), registration/relative orientation with ICP (2.4), and different methods of adjustment and deformation analysis (2.5-2.7). The paper ends with conclusions.

Figure 1: Points from the first scan, representing the lock, colored by the RGB values as photographed by the scanner's internal camera. At the bottom some scan shadows are visible.

2. List of methods

2.1. Segmentation

Segmentation groups points, which have under a given homogeneity criterion similar properties, into segments. A short overview on segmentation can be found in [8]. The method applied here follows the region growing approach for extracting planes. First, in each point an initial normal vector is estimated from its neighbors by fitting of a plane.[1] Points with a large r.m.s.e. are discarded from the beginning, because they are more likely to be single points, or on surfaces with a very small extent. Planes are grown, starting with the initial normal vector

[1] For determining the plane parameters we compute the matrix of second moments of the points reduced to their center of gravity. The eigenvector to the smallest eigenvalue of this matrix is the plane normal.

and position of the seed point. Neighboring points are accepted if they are i) below a threshold distance to this plane, and ii) the angle between plane normal vector and initial normal vector is below a threshold. After adding a point, the plane is determined anew by adjustment of all accepted points. If no more points can be added to a segment, the next segment is initiated with a new seed point. An example of the segmentation for one scan can be seen in Fig. 2.

2.2. Direct comparison of observed points

If we assume that the scanner's position is fixed between two scans we can directly compare the two scans obtained, as follows. The emittance direction of the points is completely parameterized by the horizontal angle, β, and the vertical angle, ζ, of emittance and is the same for the two different scans. Moreover, these two angles β and ζ can be reconstructed from the *xyz* coordinates by converting the lather in polar coordinates. Now the remaining coordinate, *R*, in the polar coordinate system, corresponds directly to the observation, that is, by comparing the two ranges $R_p(1)$ and $R_p(2)$ at scan configuration $p=(\beta,\zeta)$ we can find possible deformations as $R_p(1) - R_p(2) = n(p) + d(p) + s(p)$, where $n(p)$ denotes the measurement noise, $d(p)$ deformation, and $s(p)$ systematic errors.

For a single point *p* it is not possible to determine the values of the three contributions to $R_p(1) - R_p(2)$. Therefore a larger set of differences is considered simultaneously. If the differences consist mainly of random noise, the distribution of the differences will be close to normal. A (local) shift in the data however may indicate either a deformation or some systematic error. This can be checked for by selecting parts of the data set that represent stable features. For such features a shift will indicate a systematic error. An indication for the direction of the shift can be obtained by an analysis as described in the following.

2.3. Analysis of movement with normal vectors

To check whether there is stationarity between two scans, or not, an analysis with manual interpretation is proposed. For each point *p* in scan 1 its normal n_p is computed by determining an adjusting plane through some neighbouring points of point *p* in scan 1 and taking its normal. For a point *b* in scan 2 the closest point in scan 1, say point *a*, is searched. The projection of the difference vector *b-a* on the normal n_a can be built.[2] This vector indicates for each point the direction of movement and its magnitude.

This procedure can be applied to all points, and if the length of these vectors is random throughout the entire data set it indicates stationarity. Otherwise, groups of nearby vectors with similar direction and length indicate movement of objects between the epochs. This procedure can be applied favorably to segments (see Sec. 2.1). Segments represent features, e.g. house walls, and an averaged shift vector can be computed and visualized per feature.

For this method it is not necessary, that the two scans were taken from the same position. However, they have to be in the same coordinate system, or this has to be assumed.

2.4. Registration with ICP

If direct comparison (Sec 2.2) is not possible, because of changes in the scan position, comparison can be made possible by transforming the different scans into one superior

[2] This is similar to the first step of the ICP, especially to its ICT (iterative closest tangent plane) variant.

coordinate system. For this purpose we use the Iterative Closest Point (ICP) method [9]. It works on two scans, transforming the point cloud of the second scan into the coordinate system of the first. In the implementation used, the corresponding (closest) point in the first scan is computed for every point of the second scan, and the distance within each point pair is used for sorting the correspondences. The correspondences with the shortest distances, specified by a fixed percentage, e.g. 20%, are used to determine the six transformation parameters (shift and rotation) for minimizing the distance between corresponding points. Iteration end is declared, if the sum of squared distances does not become smaller anymore.

2.5. Adjustment to surface models

In the segmentation algorithm (Sec 2.1), but also in later steps of deformation analysis it is necessary to find a mathematical parameterization for planar patches (e.g., segments). The model parameters $\hat{x} = (a, b, c)$ for the planar model $x\ a + y\ b + c = z$ and the model residuals $\hat{e}$ can be found by writing

$$A = \begin{pmatrix} x_1 & y_1 & 1 \\ \vdots & \vdots & \vdots \\ x_n & y_n & 1 \end{pmatrix}, \quad y = \begin{pmatrix} z_1 \\ \vdots \\ z_n \end{pmatrix}, \quad Q_y = \sigma^2 I_n \ ,$$

and putting $\hat{x} = (A^T Q_y^{-1} A)^{-1} A^T Q_y^{-1} y$ and $\hat{e} = y - A\hat{x}$. The covariance matrix of the observations Q_y is here an identity matrix multiplied with the variance σ^2 which is the same for all observations. The covariances of the unknowns are obtained from the propagation law: $Q_{\hat{x}} = (A^T Q_y^{-1} A)^{-1}$. The spread of the resulting residual values $\hat{e}$ can be used as an indication for the model fit. If the model fits prefect, the residuals are normally distributed while there is no spatial correlation between the residuals. The correlation can be checked for by a variogram/covariance analysis. If there is no correlation, the variogram should only yield a pure nugget effect, that is, the variogram is approximately a straight line, and its offset corresponds to the noise level.

2.6. Adjustment to point models

For detecting small bumps or irregularities within a segment and for the purpose of point-based deformation detection a point-wise adjustment or smoothing step is applied. This means that within a segment the observations are interpolated to a regular grid. If a variogram analysis reveals local correlation, this correlation can be incorporated by using a Kriging method. If the variogram yields only a nugget effect, Kriging will be the same as taking the local average. But here it should be taken into account that the local average should be taken with respect to the local coordinates. Again this can be done by adjusting to a local plane in the way as described above: first local plane parameters $\hat{x}$ are detemined from all observations in the grid cell at hand, then adjusted coordinates $(u, v, (u, v, 1)^T \hat{x})$ are determined. Additionally to an adjusted point location we also obtain an error variance from either the Kriging procedure or from the local plane adjustment.

2.7. Deformation and systematic shift detection

After the previous steps we can assume that for a planar segment in each scan *i* we have determined the parameters $\hat{x}_i = (a_i \quad b_i \quad c_i)$ that describe the best fitting plane (or an other model). Moreover, we assume we have for each planar model a 3 by 3 covariance matrix

$Q_{\hat{x},i}$ describing the quality of the fit. For corresponding planes in the 2 epochs we can find an adjusting plane $ax + by + c = z$ by using the individual plane parameters and covariance matrices as follows. With I_3 as 3 by 3 identity matrix, we write

$$A = \begin{pmatrix} I_3 \\ I_3 \end{pmatrix},\ y = (a_1 \quad b_1 \quad c_1 \quad a_2 \quad b_2 \quad c_2)^T,\ x = (a \quad b \quad c),\ Q_y = \begin{pmatrix} Q_{\hat{x},1} & 0 \\ 0 & Q_{\hat{x},2} \end{pmatrix}$$

and find the parameters of the common plane $\hat{x} = (a \quad b \quad c)$ in the same way as above. An indication for the model fit is given by the test statistic $T = \hat{e}^T Q_y \hat{e} / (m-k)$ where m=6 is the number of observations and k=3 is the number of unknowns. The residuals $\hat{e}$ are defined as above. The test statistic T is often used to test whether the A-model fits to the observations. In this case this would mean that we test if the two planes in the single epochs show deformation or if they are stable, i.e. no significant difference in the parameters occurs. This test statistic for a stability test can be tested in a standard testing procedure [10], against a critical value k_α, where α denotes the level of significance of the test.

3. Data analysis

Fig. 1 shows the point cloud of the lock. It shows the area of interest where deformation shall be studied, but the data acquired by the scanner reaches from ranges of 3m to 100m. The scanner was positioned on the right side of the lock. The left side wall of the lock is visible in all scans as well.

3.1. Direct comparison of observed points

As first investigation the two scans from the same position were directly compared point wise as described in Sec. 2.2. An image of the differences is shown in Fig. 2, showing range differences for points with the same angles β (horizontal axis in the image) and ζ (vertical axis). It can be seen that the left part of the left lock door shows a very big difference in range between the two scans. The reason is that it was actually moving during the second scan. However, the light grey tone at the left of the right lock door may indicate a deformation due to water pressure. The image is, nevertheless, hard to interpret because of the noise that is dominating the entire scene. In the background (black ellipse) shifts can be observed between connected surfaces hit by the laser signal. This indicates possible systematic errors or change of coordinate systems between the two scans.

3.2. Scan segmentation results

Fur further processing points were aggregated into bigger, homogeneous structures, i.e. segmentation was performed. The method described in Sec. 2.1 yields segments as shown in Fig. 3. Points not belonging to any other segment form a one-point-segment. By applying a threshold to the segment size (e.g. 1000 points), the more significant segments can be selected. The steel plates of the lock are forming one segment each. The number of points in these segments is typically 10000. With segment extents of 1.5m-2m by 1m this corresponds to point densities in the order of one point per cm^2.

3.3. Normal analysis and coordinate system transformations

In Fig. 2 shifts could be observed in the points of a house wall between scan 1 and 2. This calls for an analysis of the stability of the entire scene. A set of segments that is horizontal,

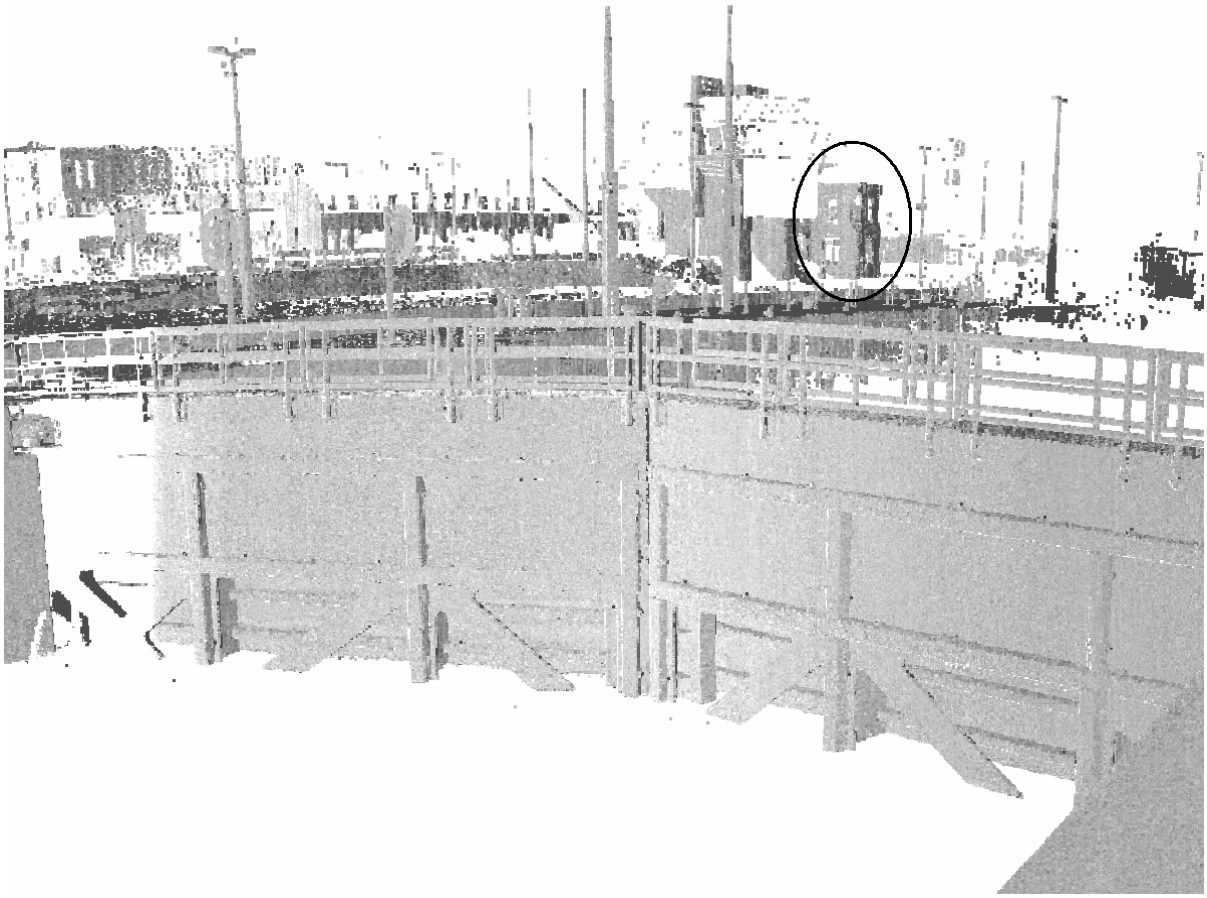

Figure 2: Signed differences in range between Scan 2 and Scan 1 using a direct comparison. Light grey tones indicate a positive difference exceeding 3cm (i.e. the points are further away from the scanner in Scan 2 than in Scan 1), while dark grey is used for negative differences of more then 3cm. Medium grey indicates no movement.

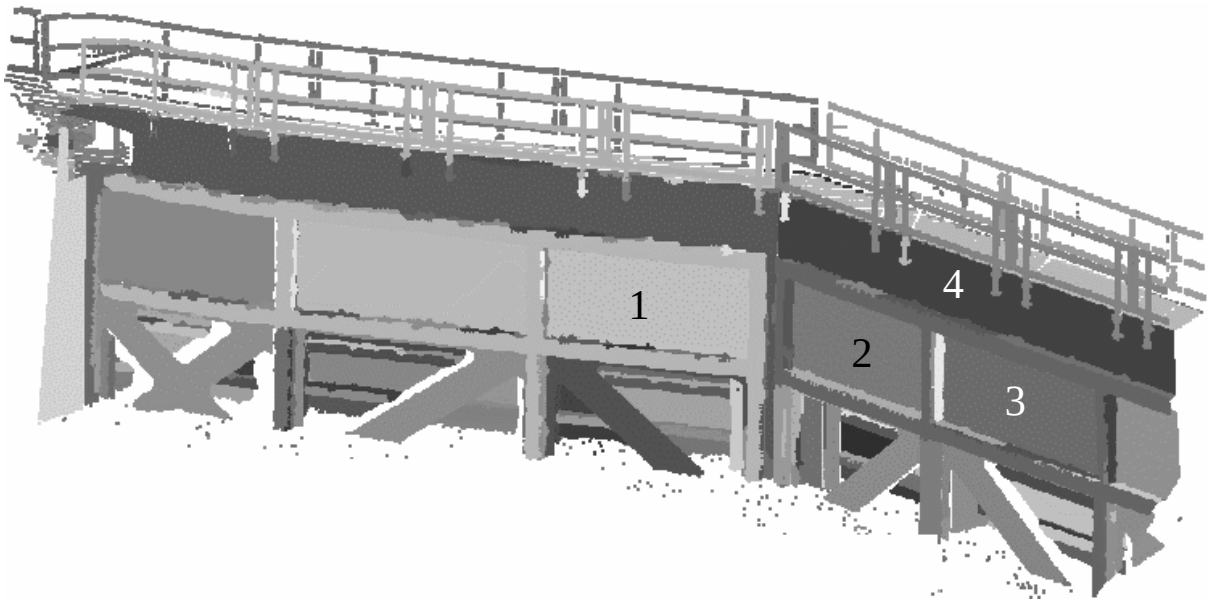

Figure 3: Segmentation of the lock data, different segments correspond to different grey tones.

parallel and orthogonal to the lock side walls was chosen an analyzed as described in Sec. 2.3. The ground close to the scanner showed a systematic upward shift of 0.3mm between the two scans. The side wall of the lock showed a sideward movement of 1.4mm between the two scans. The left wall of the lock "moved" inward. A segment orthogonal to the lock side wall, and therefore with an orientation similar to the lock doors showed a movement of -1.4mm, i.e. away from the scanner from scan 1 to 2. Objects, i.e. planes further away showed similar movements with somewhat larger offsets (up to 6mm).

These values are within the accuracy specifications for a single measurement. However, these offsets are averaged values and the random error component can be assumed to be reduced. At this point it is not clear what the cause for these movements was. Possible explanations are given in the following list.

- The scanner was moved (and rotated) between the two scans (although care was taken not to touch the device during the measurement mission).
- The environmental forces (especially wind, which was strong during scanning) caused a rotation of the scan head during the scans. This leads to not uniform distortions in the data.
- The position of the measurement was not stable and moved together with other parts of the lock due to the water pressure on the lock side walls.
- Systematic errors in the device caused the observed distortions. Especially repeatability of measurements, e.g. of the mirror position, may not be aimed to go below 2mm, which is a third of the specified measurement accuracy.

Applying ICP (Sec. 2.4) to bring the data into one common coordinate system was performed test-wise. The points on the lock were removed before, because deformations were expected there, and they would have influenced the result and compensated effects of deformation on the lock doors. The translation vector was small, i.e. in the magnitude of 3mm, and the same applies to the rotation values. Performing the normal vector analysis after the registration did not show improvement in the offset values. Therefore it was decided to continue with the data without extra registration and consider systematic errors in the magnitude of 2mm, i.e. the shifts observed between planes next to the lock doors.

3.4. Analysis of single epoch lock segment planes

In a previous step segmentation was performed for automatically selecting planar areas. However, in segmentation the validity of the model was not checked as the aim lies rather in grouping points then detailed data analysis. This analysis is described for one segment of the lock door here, but the other segment show similar behavior. A plane was fitted to the points of one segment and the residuals are shown color encoded in Fig. 4, left. The r.m.s. value of the residuals is 3mm, and the segment contained 10144 points, over an area of 1.5m by 1m. The distance of the segment points to the scanner was between 10m and 20m.

While the random errors are smaller than what could be expected from the nominal measurement accuracy their distribution appear to be not totally random. The inner part of the plane exhibits negative residuals whereas the upper right corner shows positive residuals. For analyzing this local variability a variogram of the residuals was computed (Fig. 4, middle). As the variogram shows only a nugget component, it can be concluded that there is no spatial correlation in the data above the noise level. Nevertheless, there is apparently a small variation in the model that should not be neglected as it would be the case by choosing one plane model for the entire segment. The variogram analysis justifies taking a simple average in a certain neighborhood as compared to more elaborate techniques as kriging.

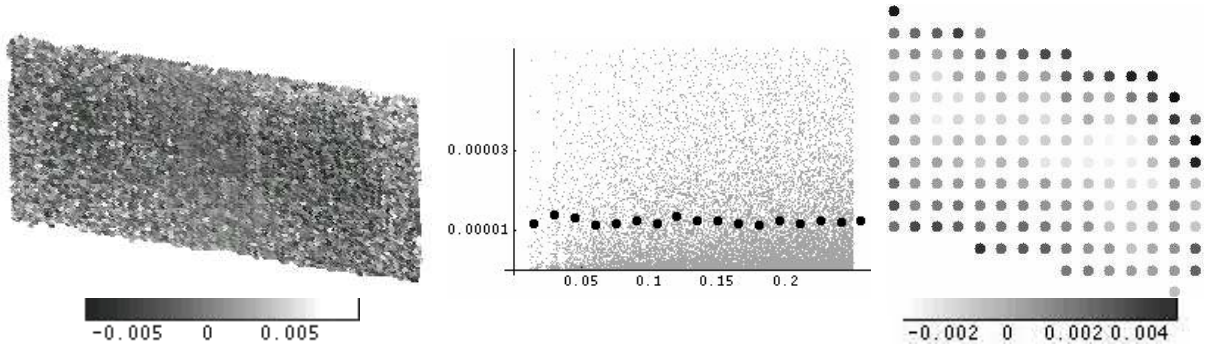

Figure 4: Analysis of one segment (number 2 in Fig. 3). Left the residuals are shown. Brighter tones refer to positive residuals of 5mm, and darker tones refer to negative residuals of 5mm. In the middle a scatter variogram (dot markers) and variogram (big filled circles) of the residuals is shown (units are m and m^2, respectively). Right the residuals are shown after averaging in a regular raster.

A regular raster with an edge length of 12cm was laid out in the xy-plane, which is near parallel to the plane of the lock doors. In each cell the residuals were averaged by taking the mean value. This clearly reveals a structure within the segment which is in the order of -2mm to 2mm (Fig. 4, right). The individual r.m.s. residuals per cell are smaller than the r.m.s. residual for the entire segment, but only by 10% on average.

Analysing the segment in the second epoch with the same method shows the same pattern as fin Fig. 4, right.

While the question for the best edge length of the raster is still not resolved, it is clearly demonstrated that this model of the lock part captures the relevant information and at the same time reduces the noise.

3.5. Deformation between scan 1 and 2

For comparing the two epochs models as derived in Sec. 3.4 are used. In the first test the planes fitted to point cloud from an entire segment were compared between the two epochs. From the four segments shown in Fig. 3, the lower test values – indicating stability – are those of segments 1 and 3, whereas the higher test values – indicating movement – are those of segment 2 and 4. The test values of segments 1 and 3 are smaller by a factor 4 than those of segments 2 and 4. While this is a first indication of deformations, analysis in the previous section has shown that the plane model is not appropriate for an entire segment and analysis for smaller regions is more appropriate.

Like shown in Fig. 4, right, the area of one segment was split up into raster cells of equal size. The edge length of the raster was chosen to be 5cm, which leads to roughly 10 points per cell. To the point set within each cell a plane was fitted. For later comparison the “height” in the middle point of the adjusted plane in each cell was stored. The accuracy σ of the measurements was taken to be 6mm, the nominal measurement accuracy. After doing this for both epochs and obtaining the covariance matrices for each set of plane parameters deformation analysis can be performed as described in Sec. 2.7. This provides one test statistic for each cell. These values reach up to 20 and are shown in Fig. 5, left. All together 1678 tests were computed.

They can be checked against the critical value using the χ^2-distribution with 3 degrees of freedom and taking a significance level of the test of e.g. 5%, which corresponds to 7.81. With this critical value 1234 cells were accepted, i.e. found to be stable, whereas 444 cells were rejected, i.e. a movement was detected with a significance level of 5%. The differences in "height" for all cells range from 0mm to 2cm. In the stable cells the differences are from 0mm to 2cm, whereas the moving cells show deviations from 9mm to 21mm. This shows the strength of statistical deformation analysis. While a simple threshold on the value of the height-difference does not take the accuracy and redundancy into account, statistical deformation analysis does. A histogram of the distances for the stable and moving cells is given in Fig. 6.

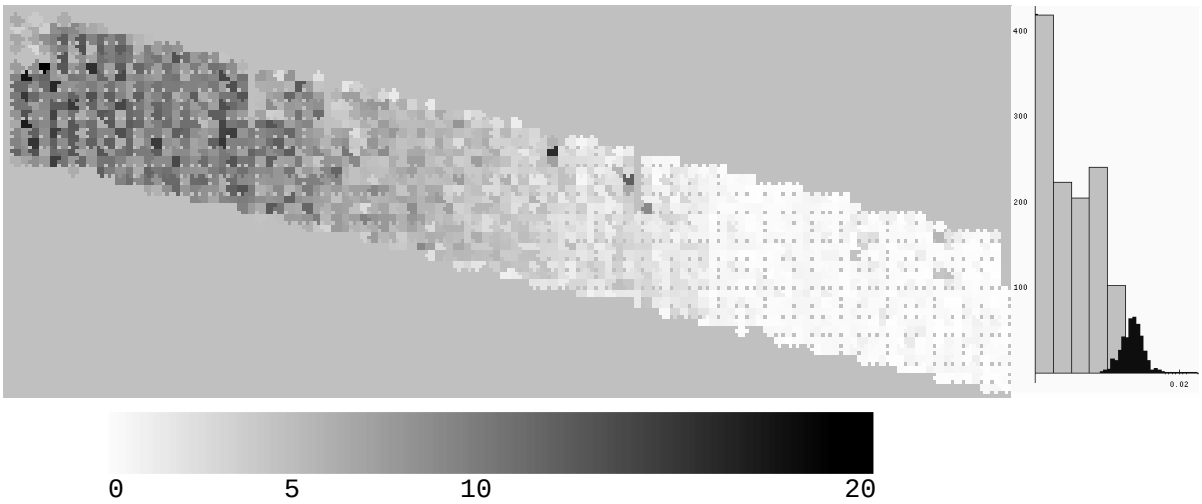

Figure 5: Left: Test statistics for a plate of the right lock door (segment 4). The test statistics are plotted grey value encoded for each raster cell. Right: Histogram of the height differences for accepted, i.e. stationary, cells in light gray, and of the rejected cells in black. The horizontal ranges from 0 to 2cm.

4. Conclusions and further research

In this paper we analyzed terrestrial laser scans from a sea lock. The final aim is to detect deformation which may only be a few millimeter in size and therefore below the nominal single point measurement accuracy. It was possible to detect deformation in the order of 9mm with a certainty of 95%. From our analysis we draw the following conclusions.

Leica claims an accuracy of 6mm at 50m for the Leica HDS2500. Analysis of plane fitting to segments lead to a measurement noise of 3mm. At the same time, a systematic error of 2mm was detected between two epochs that could not be explained. We draw the conclusion that the measurement process has to be studied further. Analysis of incidence angle, intensity of the backscattered pulse, and repeated measurements in a better controlled setting, will help in separating random and systematic components of the measurement error.

Our study shows that even a very noisy set of residuals with respect to a fitted plane can reveal structures in the order of a few mm. It is at this point not clear, if these structures are due to systematic measurement errors or features of the scanned objects. The same structures were found in both epochs.

Deformations for areas of 5cm by 5cm with a size as small as 9mm could be found with a test significance of 5% (probability of type I errors). The optimal cell size has not been studied in the project described here, and remains a subject of future investigations. It would also be of interest to develop a testing method that exploits the strong spatial correlation in the local test statistic, as visible in Fig. 5.

Statistical deformation analysis proved to be a tool superior to simple thresholding on differences. This becomes clear from looking at the histogram in Fig. 5: the overlap between the stable and moving cells is due to different redundancies and point distributions within each local raster cell.

References:

[1] Thies, M., Pfeifer, N., Spiecker, H., Gorte, B.: Three-dimensional reconstruction of stems for assessment of taper, sweep and lean based on laser scanning of standing trees. Scandinavian Journal of Forest Research 19(6), pp. 571-581, 2004.

[2] Gordon, S., Lichti, D., Franke, J., Steward, M.: Measurement of structural deformation using terrestrial laser scanners. In 1st FIG International Symposium on Engineering Surveys for Construction Works and Structural Engineering, Nottingham, UK, 2004.

[3] Schulz, T., Ingensand, H.: Terrestrial laser scanning / investigation and applications for high precision scanning. In Proceedings of the FIG Working Week – The Olympic Spirit in Surveying, Athens, Greece, 2004.

[4] Lindenbergh, R., Pfeifer, N., Rabbani, T.: Accuracy analysis of the Leica HDS3000 and feasibility of tunnel deformation monitoring. In Proceedings ISPRS workshop Laserscanning ’05, Twente, The Netherlands, to appear, 2005.

[5] Schäfer, T., Weber, T., Kyrinovic, P., and Zamencnikova, M.: Deformation measurement using terrestrial laser scanning at the hydropower station of Gabcikovo. In INGEO 2004 and FIG Regional Central and Eastern European Conference on Engineering Surveying, Bratislava, Slovakia, 2004.

[6] Pfeifer, N., Lichti, D.: Terrestrial laser scanning. GIM International, 18(12), 2004.

[7] Böhler, W., Bordas Vicent, M., Marbs, A.: Investigating laser scanner accuracy. In International Archives of Photogrammetry and Remote Sensing, Vol. XXXIV, 5/C15, 2003.

[8] Vosselman, G., Gorte, B., Sithole, G., and Rabbani, T.: Recognising structure in laser scanner point clouds. In International Archives of Photogrammetry and Remote Sensing, Vol. XXXVI, 8/W2, 2004.

[9] Besl, P., McKay, N.: A method for registration of 3D shapes. IEEE Transactions on Pattern Analysis and Machine Intelligence, 14(2), 1992.

[10] Teunissen, P.: Testing theory, an introduction. Delft University Press, Delft, 2000.